Electronic supplementary information

β-Lactoglobulin nanofibrils can be assembled into nanotapes via site-specific interactions with pectin

Charith A. Hettiarachchi,[ab] Laurence D. Melton,[*ab] Duncan J. McGillivray,[abc] Simon M. Loveday,[ad] Juliet A. Gerrard,[abcef] and Martin A. K. Williams[acg]

[a]*Riddet Institute, Massey University, Private Bag 11222, Palmerston North 4442, New Zealand*

[b]*School of Chemical Sciences, University of Auckland, Private Bag 92019, Auckland 1142, New Zealand. E-mail: l.melton@auckland.ac.nz; Tel: +64 9 3737 599 ext. 86658*

[c]*MacDiarmid Institute for Advanced Materials and Nanotechnology, Wellington 6140, New Zealand*

[d]*Massey Institute of Food Science and Technology, Massey University, Private Bag 11222, Palmerston North 4442, New Zealand*

[e]*School of Biological Sciences, University of Auckland, Private Bag 92019, Auckland 1142, New Zealand*

[f]*Callaghan Innovation, PO Box 31310, Lower Hutt 5040, New Zealand*

[g]*Institute of Fundamental Sciences, Massey University, Private Bag 11222, Palmerston North 4442, New Zealand*

Sec. 1: *Ab initio* modelling of CH and MHS β-lg nanofibrils

ATSAS software suite (v2.4, EMBL, Heidelberg, Germany)[1] was used for the development of *ab initio* bead models for the CH and MHS β-lg nanofibrils (4 mg mL^{-1}; pH 2). Indirect Fourier transformation of the scattering data was done using GNOM[2] to estimate the pair-distance distance distribution function, P(r). Maximum distance (D_{max}) for the P(r) was approximated based on radius of gyration estimated from Guinier analysis, which was performed using Igor linear fit macros.[3] A number of D_{max} values near to the approximated D_{max} were trialed to select the best P(r) to be used for the *ab initio* model development. A*b initio* modelling was conducted using DAMMIF.[4] For a given sample, 10 separate models were developed using DAMMIF, and then they were compared for the most probable model, aligned, averaged and filtered using DAMAVER.[5] The final a*b initio* models obtained for CH and MHS β-lg nanofibril samples are given in Figure S1A, and a typical fit of a DAMMIF model with SAXS data is given in Figure S1B.

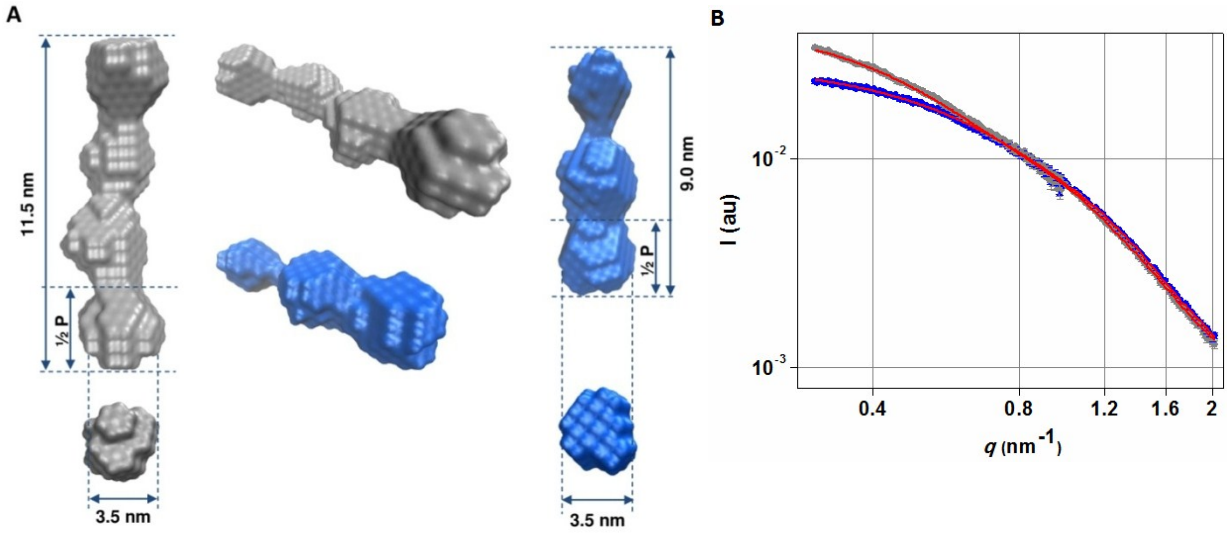

Fig. S1 Modelling the SAXS data obtained for the CH and MHS β-lg nanofibrils. (A) The final *ab initio* models obtained for the (●) CH and (●) MHS β-lg nanofibril samples. The bead radius for the CH and MHS models was automatically determined by DAMMIF to be 0.18 and 0.23 nm, respectively. Final models given here were obtained by averaging and filtering ten independent models using DAMAVER. Images were developed using VMD, v1.9.[6] (B) Typical fits of DAMMIF models with experimental data. (●) SAXS data for CH β-lg nanofibrils. (●) SAXS data for MHS β-lg nanofibrils. Continuous red lines show the scattering patterns of the respective DAMMIF models.

These models appeared to be elongated rod-like structures of a twisted nature. The cross-sectional diameter of them was 3.5 nm, and they were twisted along the long axis at ~3 nm

intervals. They were thought to represent β-lg protofilaments. Given that the inter-strand distance is 0.47 nm (Sec. 2) and the twist interval (which was considered as the half pitch, ½ P) is ~3 nm, ~13 β-strands along the protofilament would result in a full pitch (P; 360° twist). This number is lower in comparison to the number observed with typical amyloid protofilaments,[6] suggesting that the tilt angle between the adjacent β-strands is relatively higher for the β-lg protofilaments. However, conclusive evidence on the tilt-angle or the pitch cannot be obtained without performing rigid body modelling on the *ab initio* models, which is a challenging task due to a large number of different peptides involved in β-lg protofilament/nanofibril formation and the uncertainty of their sequence within the protofilaments.

Sec. 2: Two dimensional WAXD experiments

2D-WAXD was conducted at the X-ray facility of the Institute of Fundamental Sciences (IFS) at Massey University, Palmerston North, New Zealand. β-Lg nanofibril samples (20 mg mL^{-1}; pH 2) were transferred onto watchglasses and allowed to dry at 40 °C inside an air oven. The glassy film formed after complete drying of the samples was ground into a fine powder. The powders were then filled into Markröhrchen 0.5 mm thin-walled glass capillaries (Hilgenberg GmbH, Malsfeld, Germany) and diffraction data were collected for an exposure time of 15 min using a Rigaku X-ray diffractometer (Tokyo, Japan) equipped with a micro-focus rotating-anode X-ray generator (λ = 0.154nm) and a Rigaku R-AXIS IV^{++} image-plate detector. Diffraction data were also collected for native β-lg (starting material) for comparison. Figure S2 presents the 2D-WAXD patterns obtained for the CH and MHS β-lg nanofibrils and native β-lg, and they all showed reflections at 0.47 and 1.1 nm^{-1}. These reflections were well defined in both nanofibril samples in comparison to the native β-lg. Presence of these reflections in native β-lg was attributed to the availability of a calyx made of β-sheets in β-lg molecules. Other reflections present in the nanofibril samples at lower length scales were thought to be originating from salts formed due to the pH adjustment with HCl. The reflection observed at ~3 nm^{-1} in the native β-lg sample (Figure S2C, inset) was attributed to the size of monomeric β-lg molecules.

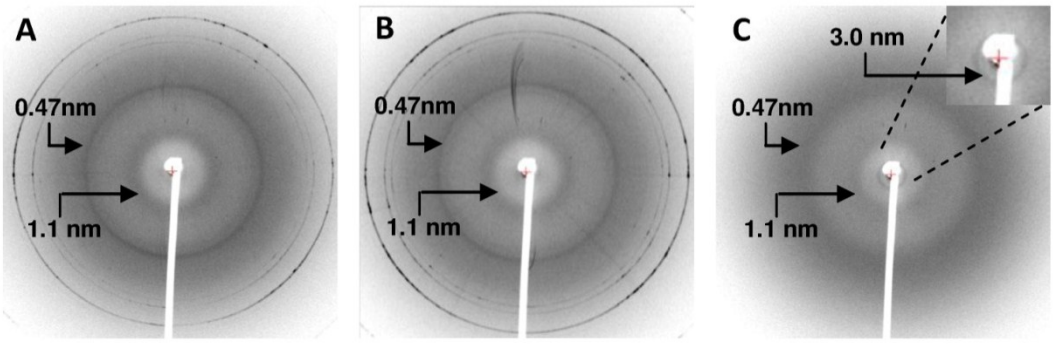

Fig. S2 Two Dimensional WAXD patterns obtained for dried powders of β-lg nanofibrils and native β-lg. (A) CH β-lg nanofibrils. (B) MHS β-lg nanofibrils. (C) Native β-lg. The inset given in C is an enlarged section of the centre of C showing the reflection at 3 nm.

Sec. 3: Verification of the activity of Endo-PG

A low methoxyl citrus pectin with a 40% DM (DM40) was dissolved in 50 mM acetate buffer (pH 4.2) to result in a concentration of 5 mg mL^{-1}. Aliquots (125 µL) obtained from this solution were mixed with 25 µL of 1:1000 diluted endo-PG solution. Dilution was carried out using the same buffer. The mixture was left overnight at the room temperature (20 °C) and then subjected to CE. Electrophorograms obtained for the endo-PG treated DM40 sample and DM40 control (without endo-PG) are illustrated in Figure S3A. Multiple peaks observed for the endo-PG treated sample were attributed to the un- or partially-methylesterified oligomeric species released by the action of endo-PG on DM40, as reported previously,[8] clearly showing the expected activity of the enzyme at 1:1000 dilution. In addition to DM40, a homogalacturonan with its DM estimated to be 97% (DM97)[9] was also treated with the 1:1000 diluted endo-PG solution to verify its substrate specificity. No possible endo-PG binding sites are expected to exist in DM97, and as expected no digestion products were detected in the endo-PG treated DM97 sample (Figure S3B).

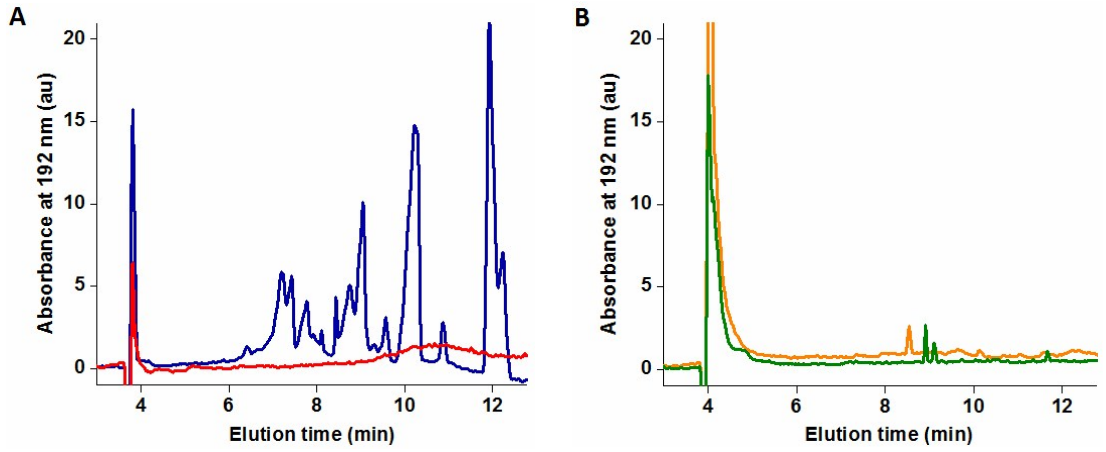

Fig. S3 Electrophorograms obtained for (A) DM40 and its endo-PG digest and (B) DM97 and its endo-PG digest. (●)DM40 + endo-PG. (●) DM40 control. (●) DM97 + endo-PG. (●) DM97 control. DM40 and DM97 solutions (5 mg mL^{-1} in acetate buffer at pH 4.2) were mixed with endo-PG solution (1:1000 dilution of the concentrate) at a volume ratio of 5:1 and kept overnight at 20 °C.

Sec. 4: Additional TEM and cryo-EM images of β-lg nanotapes

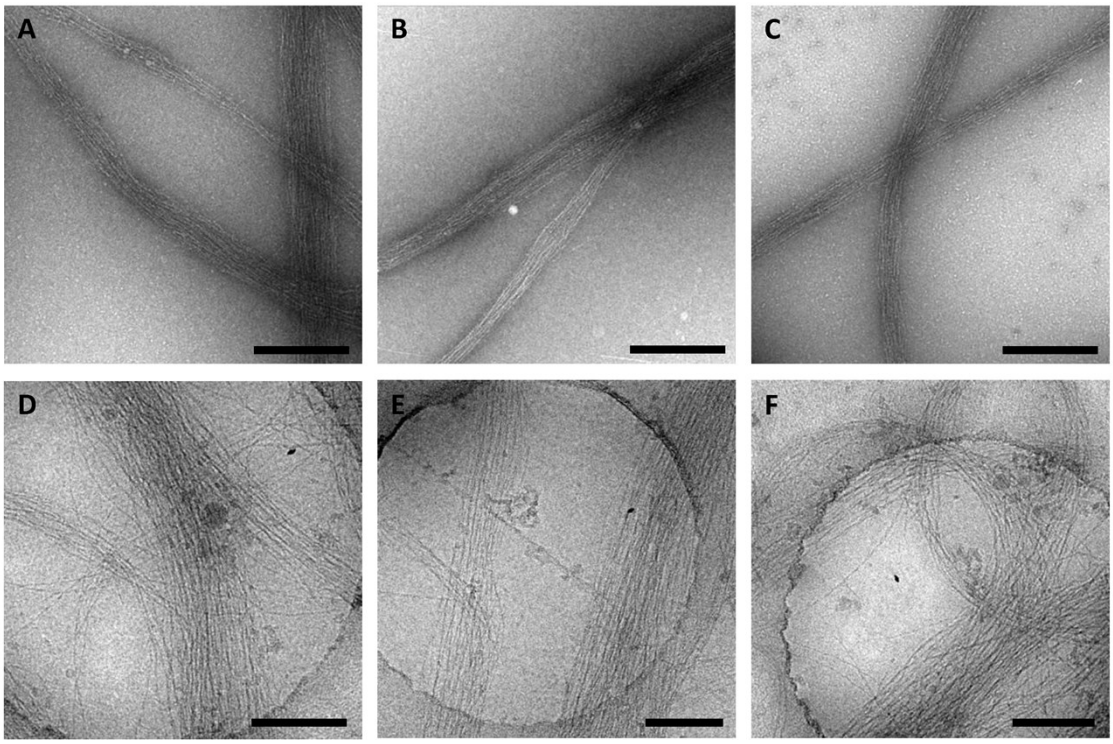

Fig. S4 Electron microscopic images obtained for 1 mg mL^{-1} CH β-lg nanofibrils + 0.05 mg mL^{-1} DM86 mixture at pH 3. (A–C) TEM images. Scale bars represent 0.5 μm. (D–F) Cryo-EM images. Scale bars represent 0.25 μm.

Sec. 5: SAXS Data obtained for the samples at two different concentrations

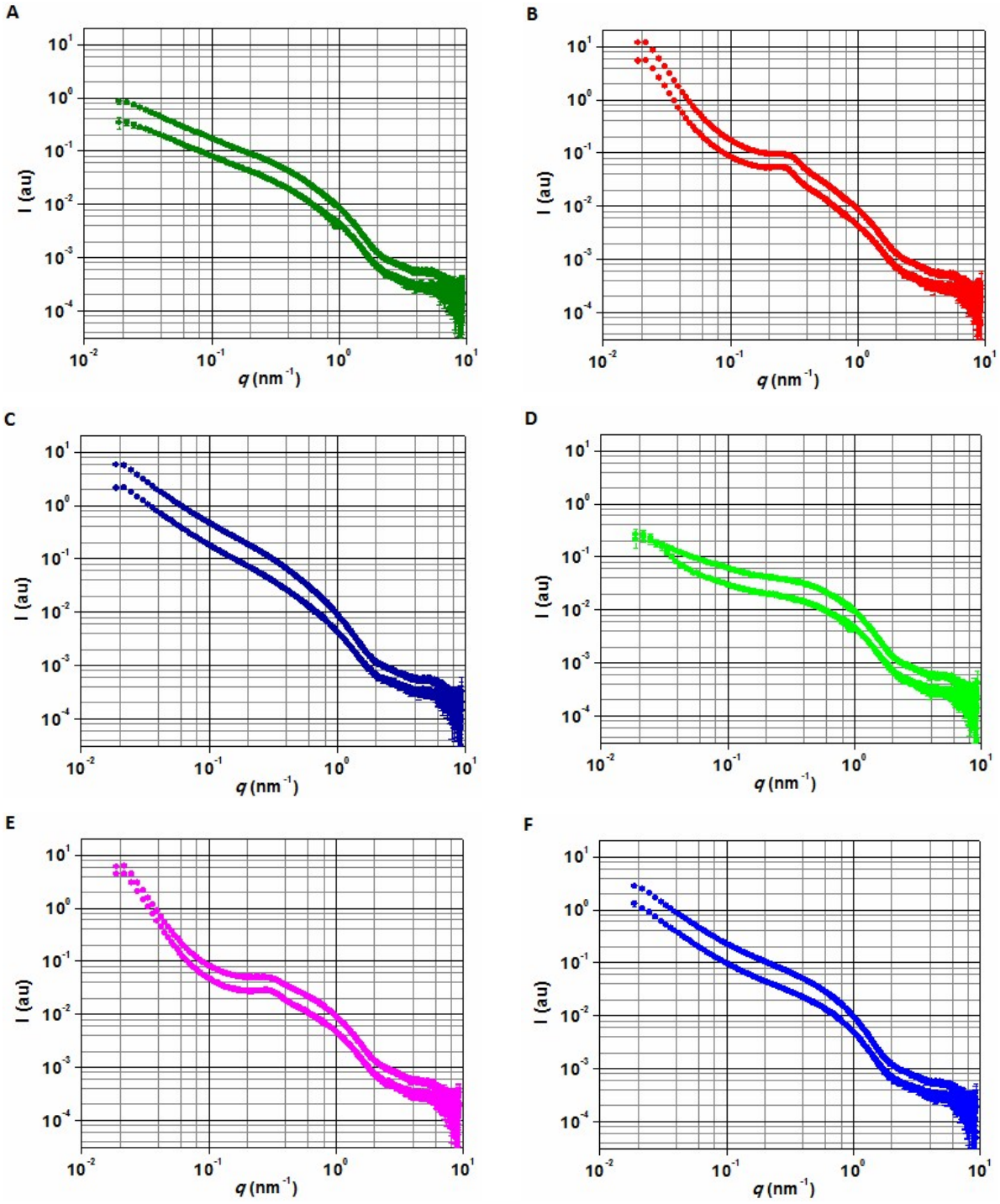

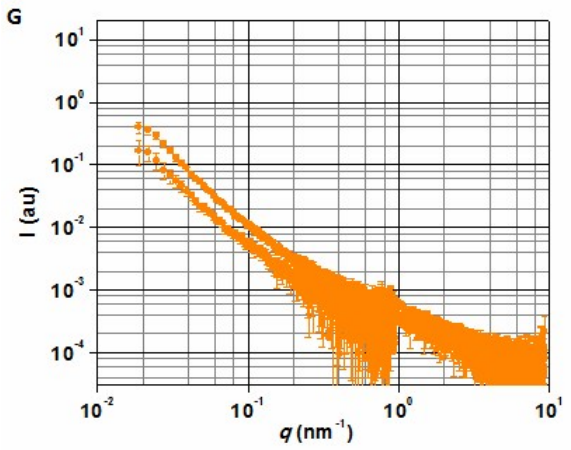

Fig. S5 Synchrotron SAXS data obtained for the samples at two different concentrations represented in I vs *q* log-log plots. (A) 2 and 4 mg mL^{-1} CH β-lg nanofibrils. (B) 2 mg mL^{-1} CH β-lg nanofibrils + 0.1 mg mL^{-1} DM86 mixture and 4 mg mL^{-1} CH β-lg nanofibrils + 0.2 mg mL^{-1} DM86 mixture. (C) 2 mg mL^{-1} CH β-lg nanofibrils + 0.1 mg mL^{-1} DM86 mixture with 100 mM NaCl and 4 mg mL^{-1} CH β-lg nanofibrils + 0.2 mg mL^{-1} DM86 mixture with 100 mM NaCl. (D) 2 and 4 mg mL^{-1} MHS β-lg nanofibrils. (E) 2 mg mL^{-1} MHS β-lg nanofibrils + 0.1 mg mL^{-1} DM86 mixture and 4 mg mL^{-1} MHS β-lg nanofibrils + 0.2 mg mL^{-1} DM86 mixture. (F) 2 mg mL^{-1} MHS β-lg nanofibrils + 0.1 mg mL^{-1} DM86 mixture with 100 mM NaCl and 4 mg mL^{-1} MHS β-lg nanofibrils + 0.2 mg mL^{-1} DM86 mixture with 100 mM NaCl. (G) 0.1 and 0.2 mg mL^{-1} DM86. In each plot, curve with the higher intensity represents the SAXS data obtained for the higher concentration.

Sec. 6: TEM images obtained for the CH β-lg nanofibrils + GalA oligomer and CH β-lg nanofibrils + GalA monomer mixtures

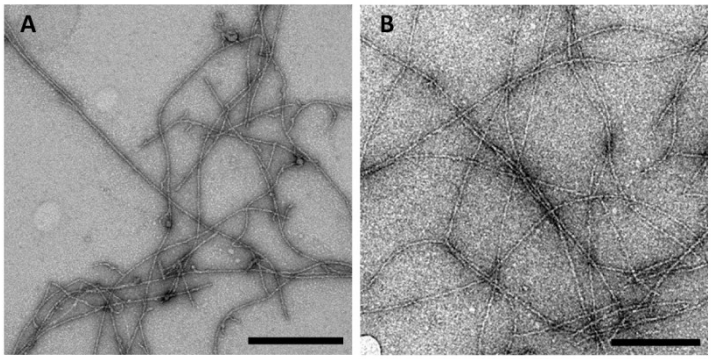

Fig. S6 TEM images of (A) 1 mg mL^{-1} CH β-lg nanofibrils + GalA oligomer mixture and (B) 1 mg mL^{-1} CH β-lg nanofibrils + GalA monomer mixtures at pH 3. The final concentration of GalA oligomers (a mixture of heptamers and octamers) and GalA monomer present in the above mixtures were equivalent to the concentration of non-methylesterified GalA units present in DM86 at 0.05 mg mL^{-1} concentration. Scale bare represent 0.5 μm.

Sec. 7: Parallel and slipped plane arrangements for the β-lg nanofibrils within a nanotape

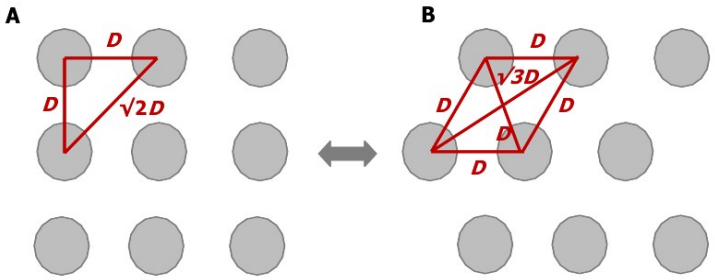

Fig. S7 Possible cross-sections for β-lg nanotapes, if they consist of multiple layers of nanofibrils. Cross-section of each nanofibril is represented by a grey circle. (A) β-Lg nanofibrils arranged in parallel planes. (B) β-Lg nanofibrils arranged in slipped planes. Spacings in between the central axes of β-lg nanofibrils are represented in *D* and its derivatives.

Sec. 8: Lower magnification TEM images obtained for the CH β-lg nanotapes

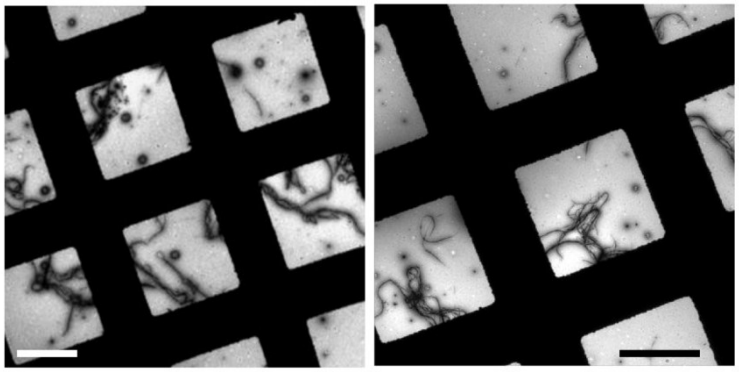

Fig. S8 TEM images obtainbed at lower magnification for 1 mg mL^{-1} CH β-lg nanofibrils + 0.05 mg mL^{-1} DM86 mixtures at pH 3. Scale bars represent 20 μm.

Sec. 9: Width distributions for the CH and MHS β-lg nanofibrils based on TEM image analysis

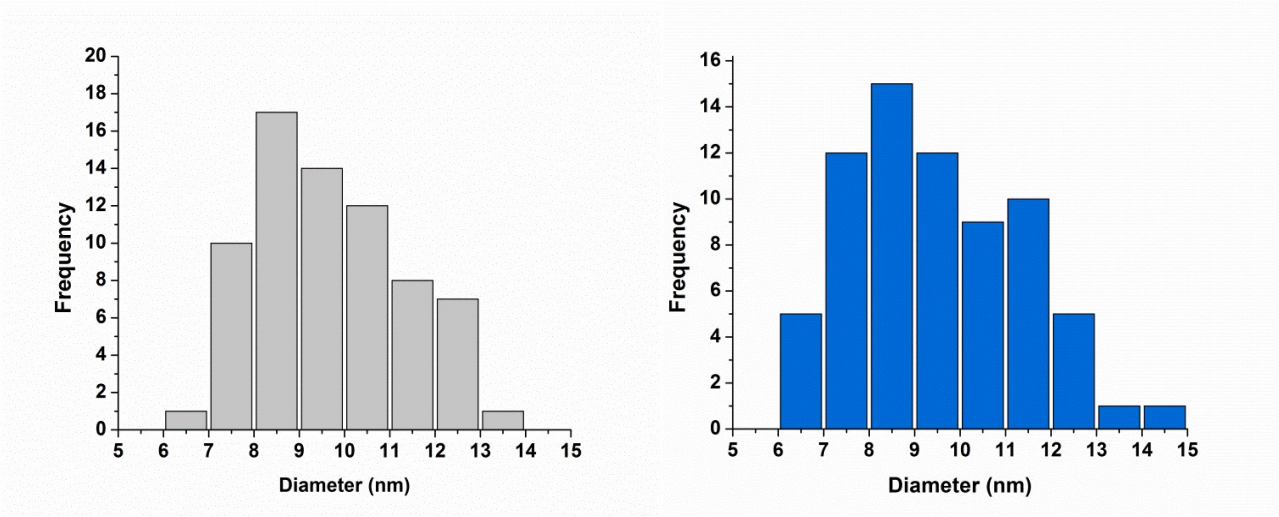

Fig. S9 Width distribution for (A) CH β-lg nanofibrils and (B) MHS β-lg nanofibrils. For each type, 70 individual nanofibrils were selected from the TEM images obtained on 4 separately prepared nanofibril samples. ImageJ software (v1.43, National Institute of Health, Bethesda, MD, USA) was used to convert pixels to nm.

Sec. 10: Calculations for the estimation of number of GalA residues distributed randomly and block-wise in DM86

The products that resulted from the endo-PG digestion of DM86 had a Mw of ~24 kDa (which is equal to half of the M_w of DM86) and a DM of ~89%. In order to rationalise this observation, it was assumed that DM86 molecules carry a block of non-methylesterified GalA residues in the middle of their backbones, with the possibility of having an additional block of non-methylesterified GalA residues at one or both ends of the chain.

Such a structure would initially be cleaved resulting in two chains of similar size with non-methylesterified GalA residues present at one or both end(s), and over time, these end regions that bind and move slowly owing to a lack of residues in some enzyme subsites, would also be cleaved by the action of endo-PG. It was assumed that the action of endo-PG on these chains is completed by the seventh day.

Given that the number of methylesterified GalA residues present in DM86 is ~192, the two homogalacturonan chains that result from the endo-PG action would comprise of ~96 methylesterified GalA residues. In order to have the measured post endo-PG DM of 89%, each chain would have to contain ~12 non-methylesterified GalA residues, together with the ~96 methylesterified GalA residues. If some of these ~12 non-methylesterified GalA residues are present at one or both ends of a chain, they would have to be originated from the non-methylesterified GalA blocks that were present in the DM86 backbone. Moreover, after the completion of endo-PG action, the minimum number of non-methylesterified GalA residues that can be left at the ends of a chain would be 1.[10] Considering the above facts, following models are proposed for the DM86 backbone (Figure S10).

A model with only one block of non-methylesterified GalA residues in the middle of the backbone seemed to be unlikely for the DM86, in which case the block size would reach ~10 residues. If a block of ~10 non-methylesterified GalA residues was available in the DM86 backbone, clear di- and tri- galacturonic acid peaks should have been present in the electrophorograms obtained for the endo-PG treated DM86.[11]

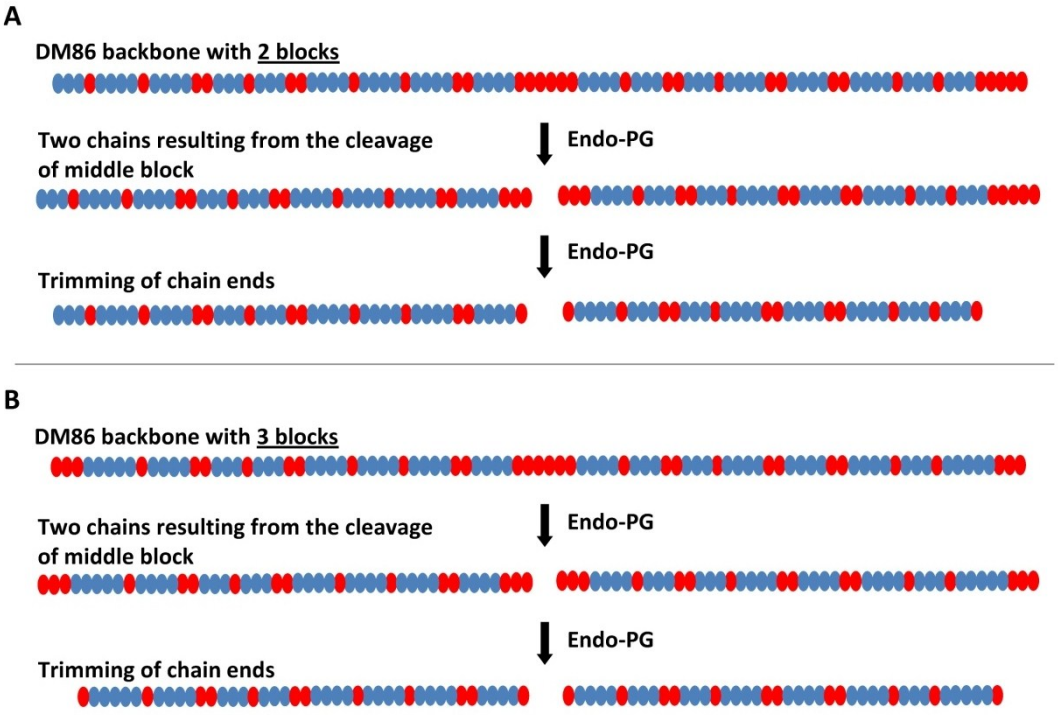

Fig. S10 Proposed models for the DM86 backbone, and the products resulting from its endo-PG cleavage. (●) Methylesterified GalA residues (not drawn in scale with the calculated numbers). (●) Non-methylesterified GalA residues (drawn equally to the calculated numbers). DM86 backbone carries ~192 methylesterified GalA residues and ~32 non-methylesterified GalA residues. Among the ~32 non-methylesterified GalA residues some are randomly distributed in singles or pairs, while the others are in blocks of ≥ 3residues. (A) DM86 backbone with 2 blocks. (B) DM86 backbone with 3 blocks. Cleavage of the middle block by endo-PG will initially result in two chains with non-methylesterified GalA residues at one or both ends, and they still have the ability to form β-lg nanotapes. Over time, the non-methylesterified GalA residues at the ends will be cleaved by the action of endo-PG leaving only one residue, and consequently they will lose the ability to form β-lg nanotapes. At the end, each chain will carry ~96 methylesterified GalA residues and ~12 non-methylesterified GalA residues giving a DM of ~89%.

References

1. M. V. Petoukhov, D. Franke, A. V. Shkumatov, G. Tria, A. G. Kikhney, M. Gajda, C. Gorba, H. D. T. Mertens, P. V. Konarev and D. I. Svergun, *J. Appl. Crystallogr.*, 2012, **45**, 342−350.
2. D. I. Svergun, *J. Appl. Crystallogr.*, 1992, **25**, 495−503.
3. S. Kline, *J. Appl. Crystallogr.*, 2006, **39**, 895−900.
4. D. Franke and D. I. Svergun, *J. Appl. Crystallogr.*, 2009, **42**, 342−346.
5. V. V. Volkov and D. I. Svergun, *J. Appl. Crystallogr.*, 2003, **36**, 860−864.
6. M. Sunde, L. C. Serpell, M. Bartlam, P. E. Fraser, M. B. Pepys and C. C. F. Blake, *J. Mol. Biol.*, 1997, **273**, 729−739.
7. W. Humphrey, A. Dalke and K. Schulten, *J. Mol. Graphics*, 1996, **14**, 33−38.
8. A. Ström and M. A. K. Williams, *Carbohydr. Res.*, 2004, **339**, 1711−1716.
9. C. A. Hettiarachchi, beta-Lactoglobulin Nanofibrils and their Interactions with Pectins, Ph.D. Thesis, University of Auckland, 2013.
10. H. C. M. Kester, D. Magaud, C. Roy, D. Anker, A. Doutheau, V. Shevchik, N. Hugouvieux-Cotte-Pattat, J. A. E. Benen and J. Visser, *J. Biol. Chem.*, 1999, **274**, 37053−37059.
11. M. A. K. Williams, A. Cucheval, A. T. Nasseri and M.-C. Ralet, *Biomacromolecules*, 2010, **11**, 1667−1675.